Journal of Visualization, Vol. 12, No. 1 (2009) 17-25

Regular Paper

Effect of Rounded Edged Dimple Arrays on the Boundary Layer Development

Mitsudharmadi, H.*, Tay, C. M. J and Tsai, H. M

* Temasek Laboratories, National University of Singapore, Engineering Drive 2 Singapore 119260, SINGAPORE.
E-mail: tslhm@nus.edu.sg (Corresponding Author)

Received 29 October 2007
Revised 31 March 2008

Abstract : The effect of a turbulent boundary layer subjected to a series of rounded edged shallow dimple arrays with dimple depth ratios, d/D of 4%, 8% and 12% were experimentally studied. Measurements show the existence of a higher flow speed region at the center of each dimple. The spanwise distribution of the mean wall shear stress immediately downstream of the centers of the last row of dimples does not vary with dimple depth, and is about 45% over that without the dimple array. Turbulence measurements and surface flow visualization shows that the flow over the shallowest dimple differs from the deeper dimples. Flow separation observed with the deeper rounded edged dimples produce similar flow structures as those from sharp edged dimples reported in the literature. However flow separation is not observed when d/D = 4% but instead two other higher speed regions either side accompany the central flow. The effects of the dimples are rapidly suppressed by the flat surfaces between of the dimples, and the flow rapidly reverts back to an unmanipulated flat boundary layer flow in these areas.

Keywords : shallow dimple, smooth edge dimple, flow control, wall shear stress, turbulent flow

1. Introduction

Early investigations of the effects of dimple cavities have focused mainly on the changes in the flow structures or heat transfer either inside or downstream of a single or multiple dimples on a channel wall (Won *et al.*, 2005; Isaev *et al.*, 2000; Ligrani *et al.*, 2001 and 2005; Ligrani, 2000; Mahmood and Ligrani, 2002). These favorable heat transfer effects have led to the proposed use of dimpled surfaces ranging from micro-scale passages for electronics cooling devices to cooling passages in large-scale turbine airfoils used for electrical power generation (Won *et al.*, 2005).

Computational studies of the flow over an isolated dimple by Isaev *et al.* (2000) reveals a complex vortex forming in the dimple due to the flow separating at the edge of the dimple. Ligrani *et al.* (2001) reported instantaneous flow patterns obtained experimentally over a dimple array consisting of 13 staggered rows of dimples in a rectangular channel. The ratio of depth to dimple diameter d/D of the dimples was 20% and three different ratios of channel height to dimple diameters H/D of 0.25, 0.50, and 1.0 were studied.

The effects of dimples on turbulent flows are strongly dependent on dimple depth and the flow Reynolds number. Recent work done by Won *et al.* (2005) shows that as the dimple depth increases, larger losses in total pressure and streamwise velocity results, accompanied by higher magnitudes of time averaged streamwise vorticity, vortex circulation, and longitudinal Reynolds normal stress. Deeper dimples produce larger and stronger vortices that increase turbulent transport in the flow.

As far as the present authors are aware, none of the previously reported literature on dimple studies (Won *et al.*, 2005; Ligrani *et al.*, 2001 and 2005; Ligrani, 2000; Mahmood and Ligrani, 2002; Park *et al.*, 2004) was made with rounded edged shallow dimples with dimple depth ratios of less than 10%. These previous studies focused primarily on heat transfer, for which sharp edged deeper dimples are more likely to create stronger vortical structures to promote heat transfer.

In contrast to the above mentioned studies, the present work aims to consider the flow structures generated by rounded edged shallow dimple arrays. Shallow dimples are expected to have less impact on drag rise. Such dimples are intended to manipulate the flow field without the pronounced flow separation that is usually associated with sharp edged dimples. The effect of shallower dimple arrays on the boundary layer development is investigated here. Different rounded edged dimple arrays with d/D of 4%, 8%, and 12% are considered. The flow features around the dimples and their effects on skin friction downstream of the dimple array are presented. It should be noted that any drag reduction utilizing dimples in a turbulent boundary layer is unlike drag reduction using roughness elements such as those studied by Yamagishi and Oki (2007). These reduce drag by delaying flow separation resulting in a smaller wake. In an unseparated boundary layer, turbulent drag reduction can only be attained through a reduction in skin friction and turbulent drag generation.

2. Experimental Setup

The experiments were carried out in a blow-down low-speed wind tunnel facility with a test-section measuring 450 mm by 450 mm. Dimples were machined onto the top surface of an aluminium plate as shown in Fig. 1(a), and spans the wind tunnel width between the two side walls. This plate was positioned 100 mm above the tunnel floor.

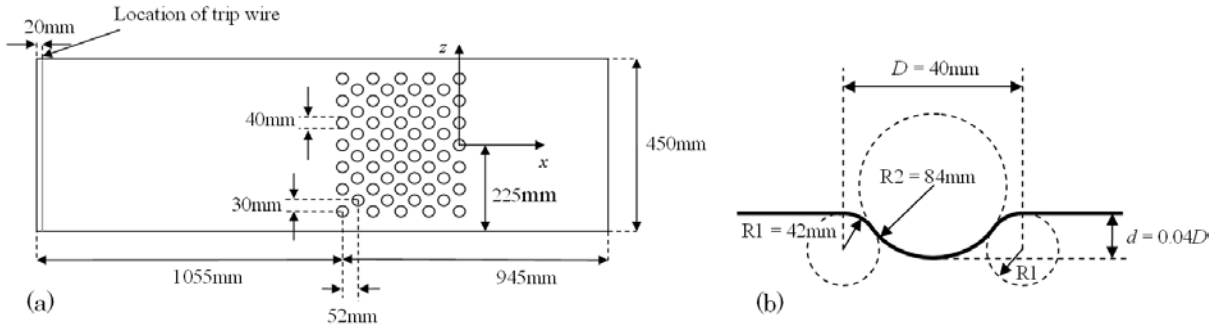

Fig. 1 (a) Sketch of dimple plated with the origin of the reference system shown.
(b) Cross-sectional view of the dimple with the dimple depth ratio of 4%.

The first 1035 mm from the leading edge of the plate was flat without any dimples. A trip wire of 1mm diameter was taped onto the plate along its entire span at a streamwise position of 20 mm downstream of a sharp leading edge to artificially trip the flow. The flat section allows the boundary layer to develop before it reaches the dimple array. The first row of dimples have their centers located at 1055 mm from the leading edge of the plate. Each dimple is 40 mm in diameter and spaced in an array consisting of a total of 59 dimples. The solidity of the dimpled surface, defined as the area occupied by the dimples as a proportion of the entire surface is 40%. The free-stream velocity was held constant at about 5.5 m/s throughout the experiments.

The cross-section of each dimple when cut along its diameter is shown in Fig. 1 (b). It consists of three sections with each section forming part of a circle. The three sections meet the flat surface of the wall as well as each other tangentially to provide a smooth continuous surface from edge to edge. The radius of curvatures R_1 and R_2 at the dimple edge and center respectively varies depending on the dimple depth ratio required. For d/D of 4% shown in Fig. 1 (b), R_1 is 42 mm and R_2 is 84 mm. The ratio of R_1:R_2 is kept constant at 1:2 for all dimple depths. The diameter D is measured between the points where the curved edges meet the surrounding wall tangentially, and is 40mm for all cases. These dimpled plates can also be replaced with another plate that is completely flat and without dimples to allow comparison of the flow with and without dimples.

Hot wire measurements were made using a boundary layer hot-wire probe operated in Constant Temperature mode (CTA). Hot wire data sampled at 6 kHz for 2^{17} data points for each time history were collected by a data acquisition board and stored for processing. The probe was regularly calibrated against a pitot-static tube placed next to it in the free stream above the aluminium plate. This pitot-static tube was removed during the actual experimental run. The hot-wire probe was positioned by a computer controlled stepper motor traverse mechanism that can be moved both in the spanwise and vertical directions to measure the velocity profiles at various spanwise positions.

Velocity measurements were taken on planes located at x/D of 0.5, 1.25, and 3.5 where x is the streamwise distance downstream of the centers of the last row of dimples. The Reynolds numbers based on the momentum thickness of the boundary layer Re_θ at these different streamwise locations ranges from 1350 to 1450 and the corresponding dimensionless boundary layer thickness δ^+ ($\delta^+ = U_\tau\delta/\nu$) ranges from 600 to 700. The momentum thicknesses used are based on measurements of the turbulent boundary layer that develops without the dimple array at the corresponding locations downstream of the leading edge.

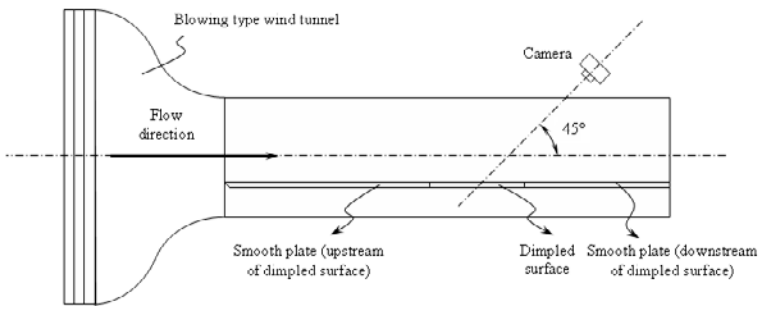

Fig. 2 Illustration of taking picture of surface visualization.

Surface flow visualizations for all three dimple depths studied were also carried out using an particle-oil mixture consisting of TiO_2 particles and a mixture of kerosene and WD40 lubrication oil. The results of these visualizations were recorded by a Nikon D100 digital camera mounted above the Perspex roof of the wind tunnel and looking down at an angle of about 45° onto the dimple array as shown in Fig. 2. To ensure that the pictures taken reliably show the final visualization image after all the solvent has evaporated sequential shots were taken at about 30-second intervals until no significant movement is observed between two subsequent shots. Sequential shots were usually conducted for a total period of about 20 minutes to ensure that all the solvent has fully evaporated.

3. Results and discussions

3.1 Hot-wire measurements

A series of velocity measurements over a smooth flat plate in place of the dimpled plate was first made. The effects of the dimple array on the turbulent boundary layer were compared against these measurements. Since the shedding or ejection of fluid is a key feature of the flow over dimples (Won *et al.*, 2005; Ligrani *et al.*, 2001 and 2005; Ligrani, 2000; Mahmood and Ligrani, 2002; Park *et al.*, 2004), the streamwise velocity field immediately downstream of the dimples is measured in an attempt to study this phenomenon. This shedding arises from the flow separating away from the surface over the upstream dimple edge (Isaev *et al.*, 2000).

The mean velocity fields for the different d/D ratios measured immediately downstream of the dimples at x/D = 0.5 are presented in Fig. 3. The dimple centers are spaced 60mm apart, equivalent to 1.5D. The contours show a depression at the location directly downstream of the dimple at z/D =0 for all dimple depths. This depression show that the flow speeds up at the center of the dimple near the wall compared to the flow at the sides of the dimple. However, this speeding up of the flow is restricted to a region no more than 4mm above the wall, corresponding to $y/\delta \approx 0.1$, or 0.1D.

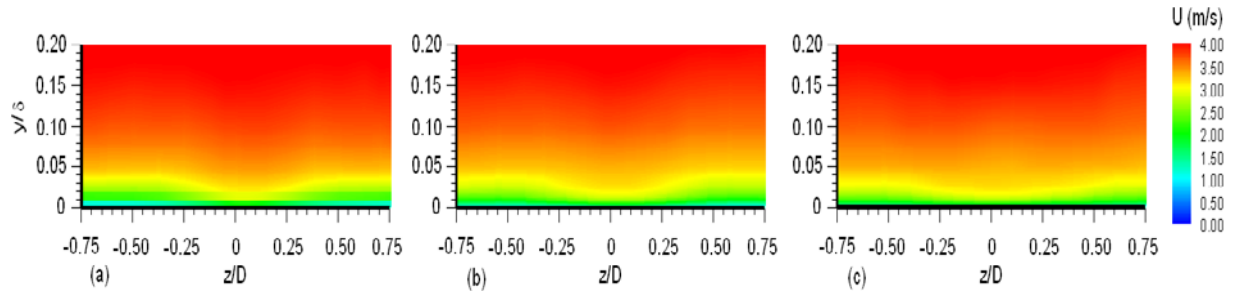

Fig. 3 Mean velocity contours at x/D = 0.5 at different dimple depth ratio (a) 4%, (b) 8%, and (c) 12%.

To estimate the local mean wall shear stress, the method used by Neuendorf and Wygnanski (1999) was applied. This method involved estimating the local mean skin friction using the local mean velocity profile near the wall. Fig. 4 illustrates typical examples of using this method for determining the wall shear stress at several spanwise locations at x/D = 0.5.

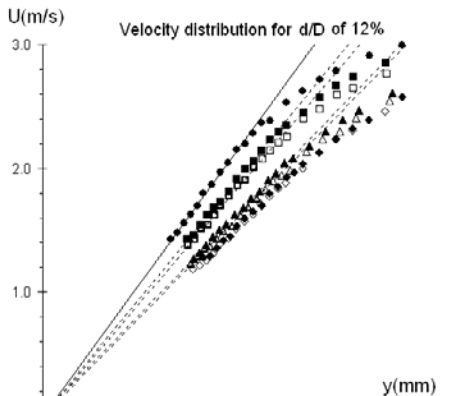

Symbol	z/D	∂U/∂y (s^{-1})	τ (N/m^2)	Uτ(m/s)
◆	-0.75	2602	0.047	0.199
▲	-0.50	2797.3	0.051	0.206
■	-0.25	3240.1	0.059	0.222
●	0.00	3661.8	0.067	0.236
▫	0.25	3137.3	0.057	0.218
△	0.50	2718.1	0.050	0.203
◇	0.75	2577.3	0.047	0.198

Fig. 4 Mean velocity distribution in near wall region for 7 spanwise locations at x/D = 0.5 for d/D of 12%.

With this method, the spanwise distribution of the mean wall shear stress at three x/D positions downstream of the dimple arrays was calculated using the velocity data and presented in Fig. 5. The spanwise variation for the flat plate case without dimples is also shown in Fig. 5 for comparison.

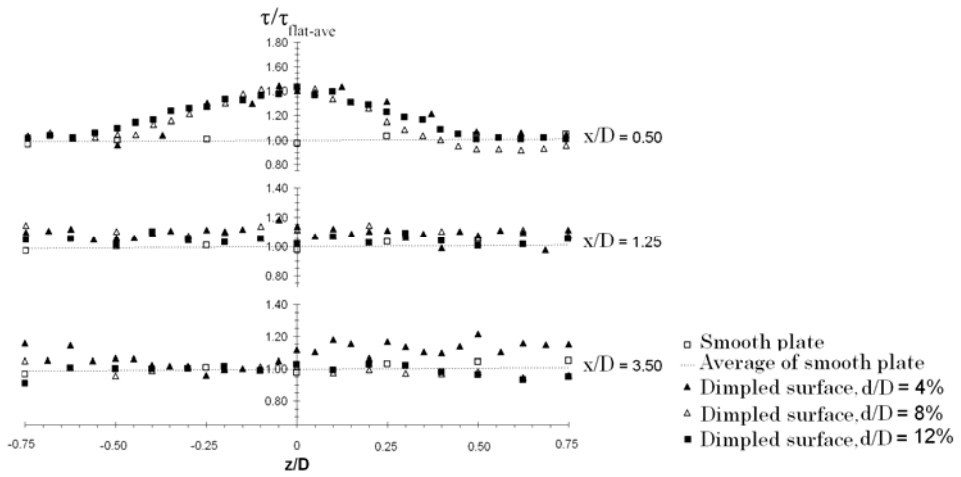

Fig. 5 Spanwise distribution of wall shear friction at x/D = 0.5, 1.25, and 3.5.

An increase in the wall shear stress by about 45% is evident at x/D = 0.5 for locations directly downstream of the centers of the last row of dimples at z/D = 0. This increase appears to be the same

for all the dimple depths studied. The higher shear stress is to be expected from the higher momentum flow in these regions shown in Fig. 3.

At either side of the dimples, the shear stress drops to a value comparable to that of a turbulent boundary layer over a flat plate. At positions measured at x/D > 0.5, no clear pattern is observed along the span. It is apparent that the effect of the dimples diminishes very quickly downstream and the shear stress everywhere becomes comparable to that of a turbulent boundary layer over a flat surface at x/D = 1.25, just 0.75 dimple diameters beyond the downstream edge of the last row of dimples.

RMS contours of the fluctuating streamwise velocity (u'_{rms}) at x/D = 0.5 are presented in Fig. 6 for all three dimple depths. For d/D = 4%, maximum u'_{rms} occurs on each side of the dimples directly downstream of the flat surfaces at z/D ≈ ±0.75. However, for the deeper dimples with d/D = 8% and 12%, maximum u'_{rms} is observed directly downstream of the dimple centers at z/D = 0, together with a pair of smaller local maxima observed at both sides of the dimple centerline at z/D ≈ ±0.75. This distinction between the shallow dimple array and the deeper dimple arrays is also observed in the vertical distribution of turbulence intensities (u'_{rms}/U_∞) along the dimple centerline shown in Fig. 7(a). It is evident that the maximum turbulence intensity increases with the dimple depth ratio (Fig. 7(b)).

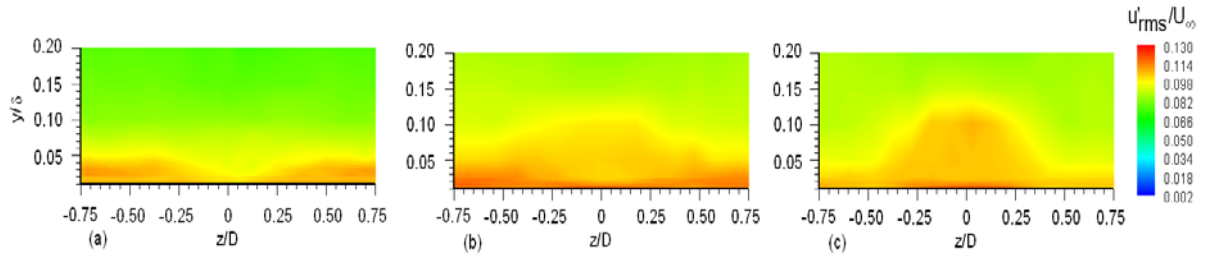

Fig. 6 Turbulent Intensity (u'_{rms}/U_∞) contours at x/D = 0.5 for different dimple depth ratio (a) 4%, (b) 8%, and (c) 12 %.

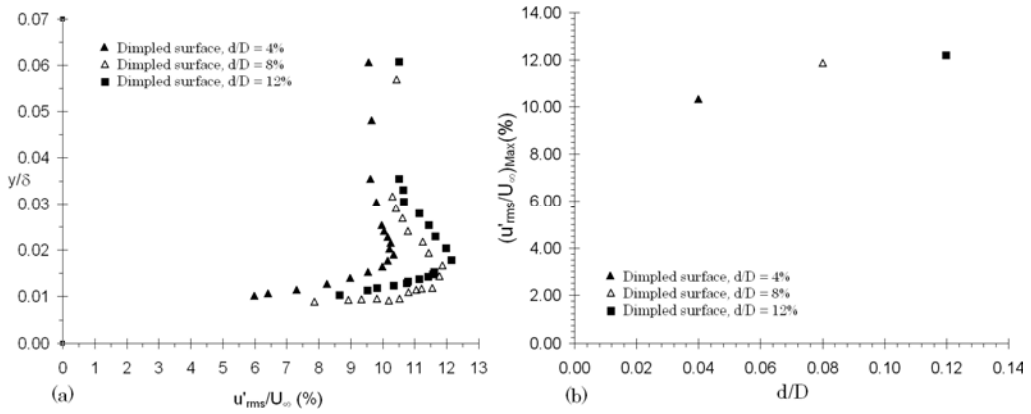

Fig. 7 (a) Turbulent Intensity (u'_{rms}/U_∞) in vertical direction at x/D = 0.5 and z/D = 0.
(b) Variation of maximum turbulent intensity as a function of d/D at x/D = 0.5 and z/D = 0.

3.2 Surface flow visualization

Measurements of the velocity field by hot wire anemometry were only carried out on the flat portions downstream of the dimple array due to the possibility that the size of the probe could affect the flow field in the dimple depression significantly. In an attempt to further understand the flow within the dimple depression, surface oil flow visualization was carried out. A mixture of kerosene, WD40 lubrication oil, and TiO_2 particles was used for this purpose.

While a less viscous mixture with more particles could be used for the shallowest dimple with d/D = 4% to show the surface flow patterns more clearly, a similar oil-particle mixture when used with the deeper dimples with d/D = 8% and 12% resulted in the mixture settling and accumulating in the dimple depressions. This accumulation may significantly alter the actual surface geometry of the

each dimple. Hence a different composition of kerosene-WD40-TiO_2 mixture with a higher viscosity had to be used with the deeper dimples.

The surface flow visualization results shown in Fig. 8 confirms the presence of the high shear stress regions in the dimple depressions, showing these areas to be swept clean of oil and particles. These regions are labeled 'A' in Fig. 8. Flow separation lines are also visible at the upstream edge of the deeper dimples with d/D = 8% and 12% and are labeled 'B' in Figs. 8b and 8c. Accumulation of particles is also observed at the upstream edges of dimples with d/D = 4%, labeled 'C' in Fig. 8a. Close inspection shows them not to be separation lines, due to the presence of visible streaks that run directly through these accumulation zones. These streaks do not cross each other and hence are an indication of the surface streamlines.

Clearly defined streaks are most distinctly seen on the flat areas between the dimples, labeled 'D' in Fig. 8. For the deeper dimples shown in Figs. 8b and 8c, these lines show the surface streamlines spreading out as the flow approaches each dimple and converging downstream of each dimple. The flow on the flat areas between the dimples appears to be mainly streamwise and no clear vortical structures seem to be apparent in these areas.

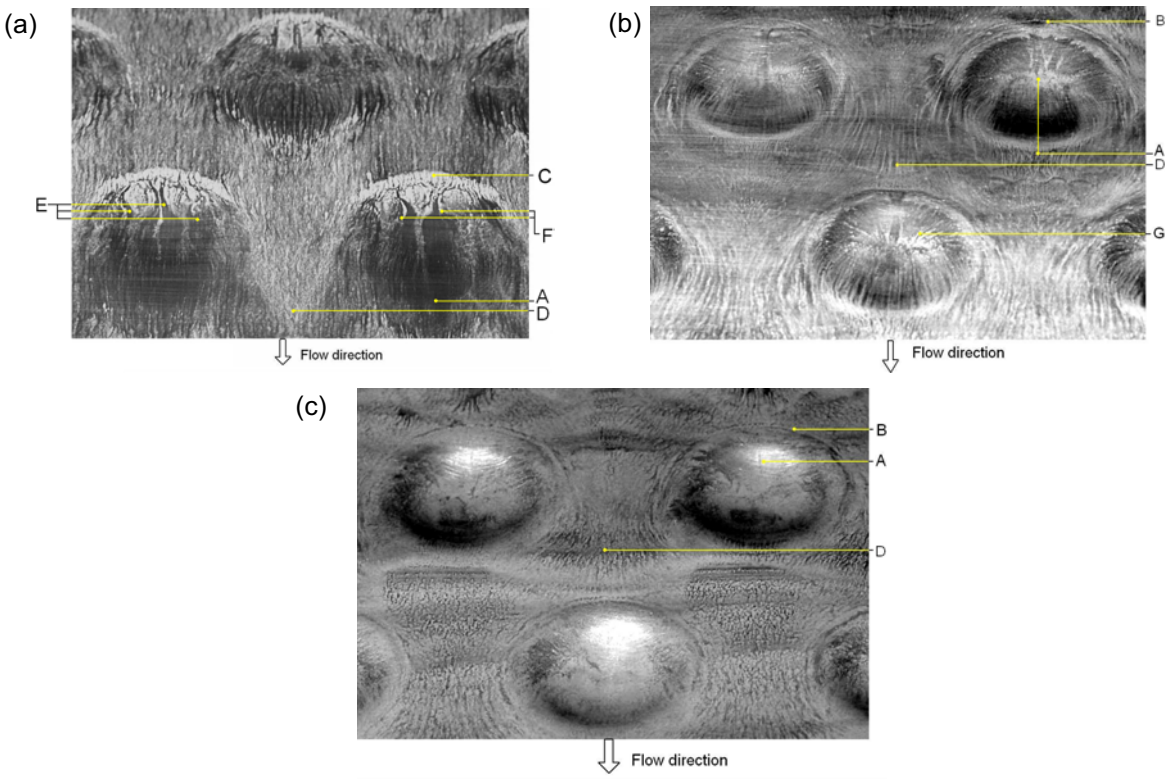

Fig. 8 Surface flow visualization results for (a) d/D = 4%, (b) d/D = 8%, (c) d/D = 12%. A: high shear stress area inside dimple, B: diverging streamlines ahead of dimples, C: accumulation of trace particles in low speed area, D: surface streamlines of low speed areas along flat surfaces, E: 'jets-like' streams, F: strong spanwise flow.

For the deeper dimples with d/D of 8% and 12%, the oil surface flow patterns are very similar. The streaks in the oil patterns of these deeper dimples suggest that there exist some flow of fluid from the center of the dimple outwards. The streaks around the perimeter of each dimple show that the features within each dimple are confined within the dimple perimeter and do not significantly affect the flow outside the dimple perimeter. The flow outside the dimple perimeter appears to simply flow around each dimple without being affected by the structures within the dimple depression significantly, at least near the wall. This is similarly suggested by the velocity measurements which show the very rapid return of the flow to one similar to a turbulent boundary layer on a flat surface within a short distance downstream of the last row of dimples.

Although the commonly reported phenomenon of fluid shedding is not observed in the present

measurements, much of what is observed in the present study concurs with what is reported in the literature. While Ligrani *et al.* (2001) reported the fluid shedding in his flow visualization study of sharp edged dimples with d/D=20%, they also reported the existence of near wall secondary flows that flow outwards from the center of the dimple. This outward secondary flow is almost continuous throughout the entire periodic cycle observed by Ligrani *et al.* (2001). It is interesting to note that while the periodic vertical ejection of fluid is observed from the center of the dimple by many researchers (eg. Won *et al.*, 2005; Ligrani *et al.*, 2001 and 2005), the depression in the velocity contours shown in Fig. 3 is more commonly associated with vertical downflow at the depression position (Bakchinov *et al.*, 1995 and Mitsudharmadi *et al.*, 2006), in this case along the dimple center.

Comparing the mean velocity contours and surface visualization obtained in the present study with those of Won *et al.* (2005) and the flow patterns observed by Ligrani *et al.* (2001) reveals why this is so. Despite flow visualization by Won *et al.* (2005) showing the periodic fluid shedding from the dimple center, this phenomenon is similarly not detected in their mean velocity contours. The contours they obtained on the other hand are similar to those obtained in the present study, showing depressions along the dimple center. Instead of showing the primary fluid ejection, these mean velocity contours actually show the underlying secondary flow patterns depicted by Ligrani *et al.* (2001). These secondary flows indeed show a downwash at the center of the dimple. The existence of these primary-secondary pairs of vortices within the dimple is similar to those observed by Ersoy and Walker (1985) in their study of a boundary layer. However in this case, the periodic nature of the upper primary vortices may explain the fact that its existence is not obvious in the mean velocity contours.

Spectral analysis (not shown for brevity) carried out using the velocity history used to obtain Fig. 3 also does not show any obvious peaks in the spectral distribution. Any peak observed is comparable to the noise surrounding it. The noise level obtained in the present study is comparable to that presented by Won *et al.* (2005), also obtained using hot-wire anemometry. However, their measurements were complimented by flow visualization and indeed without the latter, it would be difficult to determine the shedding frequency from the spectral analysis alone. It appears that the shedding frequency is not distinct, hence not clearly visible in the spectral distribution. Other methods besides single point measurements, such as flow visualization may be required to identify the shedding and determine its range of frequencies.

Isaev *et al.* (2000, 2003) observed similar flow patterns in their computational studies of sharp and rounded edged dimples. The secondary flow in the upstream half of the dimple is actually observed to flow with an upstream component both by Ligrani *et al.* (2001) and Isaev *et al.* (2000, 2003). This phenomenon of upstream flow is similarly observed in the present study (labeled '**G**' in Fig. 8b) in the deeper dimples with d/D= 8% and 12% near the upstream edge.

Besides the depressions in the mean velocity contours directly downstream of the dimple centers indicating relatively high speed regions, other similarities are also observed between the present results and those obtained by Won *et al.* (2005). Both agree that deeper dimple depths result in greater velocity fluctuations downstream of the dimples. The rms of the fluctuating velocity component (Fig. 7) is observed to increase with increasing dimple depth in the present study. These similarities are observed despite the differences in the types of dimples used in both studies. Won *et al.* (2005) used sharp edged dimples with d/D ranging from 10% to 30%, while the present study uses rounded edged dimples with d/D in the range of 4% to 12% to cover the range not previously investigated.

It appears that the type of edges, whether sharp or rounded does not play a significant influence to the resulting flow for dimples with d/D $\geq$ 8%. Since a sharp edged dimple is likely to trigger flow separation at the upstream edge, its similarity to a rounded edged dimple may imply that flow separation also occurs with the rounded edge and results in a similar flow structure for these two types of dimples. This flow separation is actually observed in the oil flow visualization results of the deeper dimples in this study with d/D $\geq$ 8%. It is possible that separation over the rounded edge may be triggered by a local adverse pressure gradient that results as the wall surface slopes away from the horizon and downwards into the dimple depression. This may explain the similarity of the deeper dimples in this study with the sharp edged dimples found in the literature. The shallowest dimples studied here with d/D = 4% may not create a pressure gradient adverse

enough to cause flow separation due to the more gently sloping surface of the shallow dimples. The flow separation that results from the deeper dimple depths may also explain the maximum u'_{rms} located along the dimple centerline in Fig. 6 for the deeper dimples but not for the shallowest dimple.

The surface flow visualization patterns for the dimples with d/D = 4% shows distinct differences from those of the deeper dimples with d/D = 8% and 12%. The differences in the flow patterns cannot be accounted for by merely the difference in the oil mixture used for the shallowest dimple. While the deeper dimples show a divergence in the streamlines ahead of the dimples and a convergence of the streamlines downstream of it, the shallowest dimples studied (d/D = 4%) shows the flow to be streamwise almost everywhere except inside the dimple depressions and very near the dimple edges.

The high speed region in the depression of the dimples with d/D = 4% clear of oil and particle traces, labeled '**A**' in Fig. 8a, occurs slightly further downstream with respect to the dimple center when compared with the deeper dimples. The flow at the upstream half of these shallow dimples appear to be more complex than that for the deeper dimples with d/D = 8% and 12%.

A large accumulation of trace particles is observed at the upstream edge of these shallow dimples as mentioned. This accumulation suggests a region of very low flow velocity and shear stress. Streaks that run through these accumulations in quasi-streamwise directions show that flow separation has not occurred here. It is therefore likely that the flow remains attached but has a very low velocity near the surface in this region.

Careful inspection of the sequential photos taken while the surface pattern is developing shows a slow spanwise flow in the region of particulate accumulation. Two relatively fast flowing jet-like streams accompany the main central stream (labeled '**E**' in Fig. 8a) flow out from this accumulation zone into the dimple depression. Strong spanwise flow is observed slightly downstream of these 'jets' and is labeled '**F**' Fig. 5a. Unlike the flow over the deeper dimples, there is also a lack of upstream flow at the upstream edges of these shallow dimples. The flow at the downstream end and outside the dimples remains largely streamwise with relatively small spanwise components.

4. Conclusion

The effect of a rounded edged shallow dimple array on the turbulent boundary layer has been experimentally studied. The study shows that the dimples affect the boundary layer only in the immediate region around it. Spanwise patterns in the velocity contours are evident only in the near wall region extending to about 0.1D above the wall. A region with high streamwise velocity immediately downstream of the center of the dimple is observed, but this diminishes within 1.25D downstream from the centers of the last row of dimples. While local maxima in the u'_{rms} occurs directly downstream of the flat portion between the dimples for all dimple depths, the deeper dimples with d/D = 8% and 12% have their global maxima located directly downstream of the dimple centers.

The distinction between the shallowest dimple array (d/D = 4%) and the deeper dimple arrays with d/D = 8% and 12% is further observed in the surface oil flow visualizations. For the deeper dimples, the flow diverges around the dimple edges, just upstream of the dimples and converges downstream just after their downstream edges. The flow within the dimple shows an outward flow of fluid along the dimple surface away from the dimple center. A high shear region is observed in the region just upstream of the dimple center.

Although a high shear stress region is similarly observed at the center of the shallowest dimples (d/D = 4%), the flow over the upstream half of the dimple is significantly more complex than that of the deeper dimples. The central high shear region shifts slightly downstream of the dimple center, and this is accompanied by two smaller high speed streaks on either side of the dimple center.

The mean shear stress immediately downstream of the dimple centerline increases about 45% compared to a turbulent boundary layer over a flat surface. However, at either side of the dimple, the mean shear stress is comparable that of a turbulent flow over a flat plate. Further downstream, the mean flow rapidly returns to that of normal turbulent boundary layer and the effects of the dimples on both the mean shear stress and flow velocity diminishes significantly.

The many similarities between the present study of the deeper rounded edged dimples and the results from sharp edged dimples found in the literature suggest that the type of dimple edge does

not affect the flow field significantly if the dimple is relatively deep, (d/D ≥ 8%). Flow separation occurs in both cases which seem to govern the flow structure over the dimple surface. This flow separation also gives rise to an increase in the u'_{rms} directly downstream of the deeper dimple centers. Only in shallow rounded edged dimples does flow separation not occur. Instead, a different and more complex flow structure forms. Further study needs to be made for these shallow rounded edged dimples to uncover the flow structures resulting from their presence and also their impact on the wall shear stress and heat transfer characteristics.

References

Bakchinov, A. A., Grek, G. R., Klingmann, B. G. B., and Kozlov, V. V., "Transition experiments in a boundary-layer with embedded streamwise vortices," Phys. Fluids, 7 (4), 820 (1995).

Ersoy, S., and Walker, J. D. a., "Viscous flow induced by counter-rotating vortices", Phys. Fluids 28 (9), 2687-2698 (1985).

Isaev, S. A., Leontiev A. I., and Baranov P. A., "Identification of self organized vortex-like structures in numerically simulated turbulent flow of a viscous incompressible liquid streaming around a dimple on a plane. Technical Phys. Lett., 26, 15 – 18 (2000).

Isaev, S. A., Leontiev A. I., Kudryavtsev N. A., Pyshnyi I. A., "The Effect of Rearrangement of the Vortex Structure on Heat Transfer under Condition of Increasing Depth of a Spherical Dimple on the Wall of a Narrow Channel," High Temperature, 41, N2, 229-232. (2003)

Ligrani, P. M., "Flow visualization and flow tracking as applied to turbine components in gas turbine engines," Measurement Science and Technology 11, 992-1006 (2000).

Ligrani, P. M., Harrison, J. L., Mahmood, G. I., and Hill, M. L., "Flow structure due to dimple depression on a channel surface," Phys. Fluids 13 (11), 3442-3451 (2001).

Ligrani, P. M., Burgess, N. K., and Won, S. Y., "Nusselt numbers and flow structure on and above a shallow dimpled surface within a channel including effects of inlet turbulence intensity level," J. Turbomachinery, 127, 321-329 (2005).

Mahmood, G. I., and Ligrani, P. M., "Heat transfer in a dimpled channel: combined influences of aspect ratio, temperature ratio, Reynolds number, and flow structure," Int. J. Heat and Mass Transfer 45, 2011-2020 (2002).

Mitsudharmadi, H., Winoto, S. H., and Shah, D. A., "Development of most amplified wavelength Görtler vortices", Phys. Fluids, 18, 014101 (2006).

Neuendorf, R., and Wygnanski, I., "On a turbulent jet flowing over a circular cylinder," J. Fluid Mech. 381, 1-25 (1999).

Won, S.Y., Zhang, Q., and Ligrani, P. M., "Comparisons of flow structure above dimpled surfaces with different dimple depths in a channel," Phys. Fluids 17, 045105 (2005).

Yamagishi, Y., and Oki, M., "Numerical simulation of flow around a circular cylinder with curved sectional grooves,"Journal of Visualization 10 (2), 179-186 (2007).

Author Profile

Hatsari Mitsudharmadi: He obtained his MEng and Ph.D degree in Mechanical Engineering from the National University of Singapore with the specialisation in Fluid Dynamics/Aerodynamics. Currently he is working as a Research Scientist at Temasek Laboratories, NUS. His research interests are fluid dynamics/aerodynamics and hot-wire anemometry.

Tay Chien Ming Jonathan: He obtained his MEng degree in Mechanical Engineering from the National University of Singapore. Subsequently he joined Temasek Laboratories where he carried out defense related research in experimental fluid dynamics. He has recently transferred and is currently working in the Department of Mechanical Engineering in NUS. His research interests include turbulent flows, aircraft aerodynamics and hot wire anemometry.

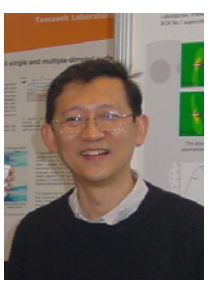

Tsai Her Mann: He received his B Sc in aeronautical engineering in 1978 from Imperial College of Science & Technology, London. Upon graduation, he did his PhD in the same college in experimental fluid mechanics. He has conducted research in Queen Mary College, London in direct and large eddy numerical simulation of turbulent flows. He has worked for the DSO National Laboratories, Singapore, where he researched and developed major codes for flow analysis and conducted studies in applied aerodynamics. Subsequently he joined Temasek Laboratories, National University of Singapore, where he started university based defense related aeronautics research work in a range of aeronautical problems from experimental flow control to flow computations and analysis for design and optimization of aerodynamic devices. To date Dr Tsai has published over 110 articles and co-edited a book on flow control.